Effect of moisture absorption on the mechanical behavior of carbon fiber/epoxy matrix composites

**E. Pérez-Pacheco · J. I. Cauich-Cupul ·
A. Valadez-González · P. J. Herrera-Franco**

Abstract A carbon fiber/epoxy unidirectional laminated composite was exposed to a humid environment and the effect of moisture absorption on the mechanical properties and failure modes was investigated. The composites were exposed to three humidity conditions, namely, 25, 55, and 95 % at a constant temperature of 25 °C. The carbon fiber–epoxy laminated composites for two different carbon fiber surface treatments were used. The results showed that the mechanical properties differ considerably for each fiber surface treatment. The application of a coupling agent enhanced the fiber-matrix adhesion and reduced dependence of the properties on humidity. The damage mechanism observed at micromechanical level was correlated to acoustic emission signals from both laminated composites. The untreated carbon fiber failure mode was attributed to fiber-matrix interfacial failure and for the silane-treated carbon fiber reinforced epoxy laminate attributed to matrix yielding followed by fiber failure with no signs of fiber-matrix interface failure for moisture contents up to 1.89 %.

E. Pérez-Pacheco
Instituto Tecnológico Superior de Calkiní en el Estado de Campeche, Av. Ah Canul SN por Carretera Federal, C.P. 24900 Calkiní, Campeche, Mexico

J. I. Cauich-Cupul · A. Valadez-González ·
P. J. Herrera-Franco (✉)
Centro de Investigación Científica de Yucatán, Unidad de Materiales, Calle 43, No. 130, Colonia Chuburná de Hidalgo, C.P. 97200 Mérida, Yucatán, Mexico
e-mail: pherrera@cicy.mx

Introduction

The carbon fiber reinforced epoxy (CFRE) in the form of laminated composites is widely used in structural applications because of their excellent performance characteristics through their design life. A critical aspect of using epoxy matrix in composites materials is their performance in moisture environments. It is well-known that the moisture has significant effects on their physical and chemical properties of epoxy matrix as well as on their final performance of composite structures especially in their long-term utilization. The absorbed water usually depresses the glass-transition temperature Tg by plasticizing the polymer network and also affects mechanical performance and long-term durability of high performance composites [1–9].

A change in moisture contents usually induces swelling that modifies the state of residual stresses in the composite material in addition to the thermal stresses produced during the curing process of the composite material [10, 11]. The resulting hygrothermal and mechanical stresses combined with each other may be sufficiently large enough to influence the failure of the laminate and thus, they should not be neglected in life time estimation.

To characterize damage evolution in traditional composite materials, many different methods have been used for many years, such as, ultrasound, scanning electron microscopy, and acoustic emission. The acoustic emission (AE) technique is a well-known non-destructive evaluation technique [12], in both research and industrial applications. It is mainly used for the detection of a wide range of microstructural failures in different materials. When a failure mechanism is activated, part of the total strain energy is dissipated as a wave that propagates from the failure source through the medium. This technique offers the possibility that it can be used even with opaque matrices, where the

points of rupture of the fibers are not visible and direct observation is not possible [13].

Mehan and Mullin [14] were the first to prompt the possibility of correlating a specific failure mechanism with its acoustic signature. Groot et al. [15] found that matrix cracking, fiber pull out, and fiber breakage in epoxy–carbon fiber composites exhibited different AE responses frequencies. Barre and Benzeggagh [16] reported that the AE amplitude varies with the different modes of fracture in glass fiber composites. Kumosa et al. [17] used the amplitude of AE events in composites to distinguish between types of damage. Low amplitude events were associated with matrix cracking and high amplitude events with fiber breakage. The influence of water absorption on the interfacial properties of aramid/epoxy composite throughout AE technique was reported by Tanaka et al. [18]. On the other hand, Godin et al. [19] studied the effects of hydrolytic aging on the AE signature of damage mechanisms occurring during tensile tests on glass fiber reinforced polyester composite. The AE technique was a successful tool to distinguish damage between aged and unaged materials through the amplitude distribution of the signals. By means of AE, Assarar et al. [20] studied the main damage mechanism induced by water absorption at the interface in glass–fiber composites materials.

In the present study, the effect of the moisture absorption on damage accumulation in carbon fiber–epoxy composites laminates for two different carbon fiber surface treatments is investigated. The level of fiber-matrix adhesion is determined with the single-fiber fragmentation test and the damage mechanism observed is correlated at macro-mechanical level and monitored with observations from an AE technique.

Materials

The composite laminates were prepared using IM7 inter-mediate-modulus carbon fibers from Hexcel Co., with a 7.0 μm average diameter. A Diglycidyl ether of Bisphenol A (DGEBA) based epoxy resin, (Epon 828 from Shell Chemical Company) was used as matrix. Nitric Acid (69–71 %), ACS and methanol ACS, both reagent grades, from J.T. Baker. Metaphenilene diamine (mPDA) ACS reagent grade was used as a curing agent, and, 3-glyci-doxypropyltrimethoxysilane ACS reagent grade from Aldrich Chemical Co as a coupling agent.

Experimental procedures

Fiber surface treatments

The carbon fiber/epoxy composite materials in form of laminates were prepared using the IM7 carbon fiber with two different surface treatments. The nomenclature used for each fiber surface treatment was the following: (1) untreated fiber (UT), referred to the carbon fiber, "as received"; and (2) silane-treated fiber (ST), referred to the IM7 fiber, but treated with nitric acid and the silane coupling agent (SCA) after removal of the commercial sizing. For the removal of the commercial sizing, the fibers were immersed and refluxed in methyl-ethyl ketone in a Kettle reactor during 12 h. Afterward, they were washed with acetone and then, with distilled water. Finally, they were dried in an oven at 120 °C for 24 h. For the SCA surface treatment, distilled water and methanol were first thoroughly mixed (50 % v/v) and the pH of the solution was measured and adjusted to 4.5 using a diluted solution of acetic acid. Then, the SCA was added to a concentration of 0.1 % (w/w) and agitated for two additional hours. Then, the fibers were immersed in the solution for 1 h, and then they were dried in an oven at 120 °C during 1 h. The nitric acid fiber surface treatment was applied to the carbon fibers after removal of the commercial sizing. The fibers were immersed in the acid (70 % purity) and refluxed for 6 h in a Kettle reactor. Afterward, the fibers were washed in distilled water and refluxed for 2 h in the reactor to remove any traces of the acid and then, they were dried in an oven at 120 °C for 2 h.

Single-fiber fragmentation test specimens (SFFT)

Single-carbon fiber/epoxy resin fragmentation test coupons were fabricated by a casting method with the aid of a silicone room temperature vulcanizing eight-cavity mold. Standard ASTM 50.8 mm long dog-bone-specimen cavities with a 3.175 mm wide by 1.587 mm thick by 25.40 mm long-gauge section were molded into a 76.20 × 203.20 × 12.70 mm silicone piece. Single fibers approximately 150 mm in length were selected by hand from a fiber bundle. Single filaments were carefully separated from the fiber tow without touching the fibers, except at the ends. Once selected, a filament was mounted in the mold and held in place with a small amount of rubber cement at the end of the sprue. Then, the epoxy resin was mixed with the curing agent at 75° C, and after degassing it was carefully poured into each cavity in the mold, taking the care of not trapping any air bubbles. The assembly was transferred to an oven (Squaroid, Model 3608-5), until the curing cycle was completed (2 h at 75 °C and 2 h at 125 °C). The specimens were tested in uniaxial tension using a micro-straining machine (MINIMAT) capable of applying enough load to the tensile coupon and fitted with a 1000 N load cell. The samples were tested using a crosshead speed of 0.02 mm/min. The load was applied and the inspection of the fiber fragmentation processed was assessed every 0.5 mm elongation intervals by counting the

number of fragments. This process was repeated until the number of fiber fragments did not increase with an increase of the applied load. At this point the test was stopped and the resulting fiber fragments were measured using an optical caliper Image XR2000. The image of the fibers was magnified using a 50× Olympus microscope objective lens (Neo Plan50) fitted to a TV camera which was connected to a TV monitor. In order to assess the interface failure process, a transmitted light polarizing microscope was configured such that there was one polarizer below and one above the test coupon for observation of the photoelastic pattern evolution as a result of the induced birefringence in the matrix.

Preparation of composite laminate

Unidirectional composite laminates were manufactured by winding carbon fiber in an aluminum frame. Afterward, the fibers were impregnated with an epoxy-mPDA mixture (the curing agent concentration was 14.5 parts by weight per hundred parts of the epoxy resin). Then, the assembly was transferred to an oven to curing cycle (Squaroid, Model 3608-5), for 2 h at 75 °C and 2 h at 125 °C) until the curing cycle was completed and keeping the sample under vacuum. The fiber volume fraction of the laminated composites was calculated according to the procedure described in ASTM D3171 [21]. The mechanical properties for tensile loadings were determined using unidirectional composite laminate specimens cut to a size of 229 mm × 13.0 mm × 2.0 mm (see Fig. 1) using a high speed diamond bench cutter according to the ASTM standard D3039-76 [22]. A Shimadzu Universal testing machine, model AG-I equipped with a 100 kN load cell and a cross-head speed of 5 mm/min.

Moisture conditioning

Both, the SFFT coupons and the laminated composite tensile test samples were conditioned to several relative humidities (RH) controlled environments (25, 55, and 95 %) at a constant temperature of 25 °C, until ready for testing. Air-tight sealed glass chambers were used as conditioning chambers. The different relative humidity environment chambers were obtained using several saturated salts and they were selected according to the recommendations given in ASTM E104-51 and ASTM E104-85 standards [23]. Potassium acetate and magnesium nitrate hexahydrate were used for the 25 % RH and 55 % RH, respectively. The 95 % RH was achieved by placing a pan with natural water inside the chamber. A digital hygrometer was place inside each chamber to measure and continuously monitor the temperature and relative humidity. The weight gain of the test coupons after exposure to the selected relative humidity environments was measured as a function of time. The humidity content was estimated using the following equation [13, 14]

$$M = \frac{M_{\mathrm{w}} - M_{\mathrm{d}}}{M_{\mathrm{d}}} \times 100, \qquad (1)$$

where M is the percentage of gained humidity, M_{w} is the weight of the wet sample, and M_{d} is the weight of the dry sample. The weight of the dry samples, i.e., the weight of the samples in the 25 % relative humidity chamber and in this case, at the beginning of the conditioning period it was observed that the samples lost weight. When the samples did not lose anymore weight, some of them were transferred to the 55 and 95 % relative humidity chambers and their weight gain was continuously monitored.

Acoustic emission (AE) measurements

The effect of the absorbed moisture on the mechanical behavior of the laminated composites was also studied by detecting the AE signals, while conducting the tensile test. The AE signals before and after moisture exposures were registered utilizing two piezoelectric transducers (see Fig. 1). Each transducer with an effective area of contact equal to 239.42 mm^2 was affixed to the tensile test coupons, and to insure good contact, vacuum silicon grease was used. A data acquisition MISTRAS 2001-AEDSP-32/16 system from Physical Acoustic Corp. with two channels was used. AE signals were monitored by two wideband transducer, preamplifier (PAC 1220A) with gain 40 dB, and filter HP 20, a fixed threshold of 40 dB and a transient waveform recording with a sampling frequency of 156.24 kHz.

Fig. 1 Unidirectional laminate specimens used to measure mechanical properties and acoustic emission signals
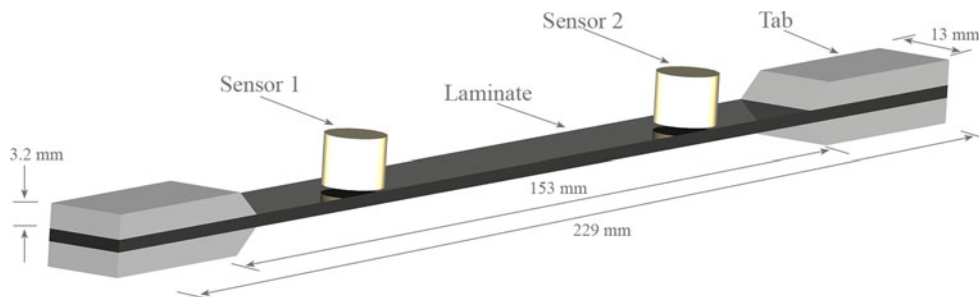
Results and discussion

Moisture absorption in CFRE laminated composites

The moisture absorption of CFRE laminates for both untreated and silane treated as a function of time is shown in Fig. 2. Similar percentage of moisture absorbed for both materials were found. For the 25 % RH, the amount of gained weight stabilizes at ~ 0.15 % after 90 days of exposure. For the 55 % RH, a larger amount of moisture is gained during the first 20 days and then it stabilizes at ~ 1 % after 90 days of exposure. For the 95 % RH, the maximum amount of absorbed water of ~ 2 % was achieved after 160 days of exposure. It was observed that the moisture absorption rate was high at the beginning of the exposure of the samples, especially during the first 20 days in both cases; afterward, the absorption rate slowly decreased until 90 days of exposure and then it stabilized to a maximum of 1 %. Only for the 95 % RH environment, the absorption rate rapidly increased during the first 20 days, and then it stabilized to a moisture gain of ~ 2 %, after 90 days. The moisture absorption behavior is similar to the previous work reported by Gupta et al. [2], Lee et al. [24] and James et al. [25]. It should be pointed out that the total moisture absorption at low relative percent humidity reaches equilibrium after approximately 70–80 days. However, these same values of absorbed moisture are attained at shorter periods of time when exposing to higher relative humidity environments.

Colombini et al. [26] proposed that there are three modes of sorption that affects moisture penetration into epoxy resin: (i) Bulk dissolution of water in the polymer network; (ii) moisture absorption onto the surface of holes that define the excess free volume of the glassy structure; and (iii) hydrogen bonding between hydrophilic groups of the polymer and water, being the last one, the dominant mode of sorption responsible for the decrease of the value for tan δ

Effect of moisture absorbed on the mechanical properties of the laminates

Figures 3 and 4 shows the tensile strength and elastic modulus for both untreated and ST CFRE matrix material as a function of moisture uptake. It should be pointed out that the absorbed moisture shown in these figures is the amount of water in the resin for any relative humidity. It is obvious from Fig. 2 that the samples exposed to the 25 % RH did not absorb more than 0.18 %; however, the samples exposed to the 55 % RH and 95 % RH absorbed almost 1.0 and 2.0 %, respectively. The behavior the tensile strength of the samples differs considerably for each fiber surface treatment (see Fig. 3). When the absorbed moisture
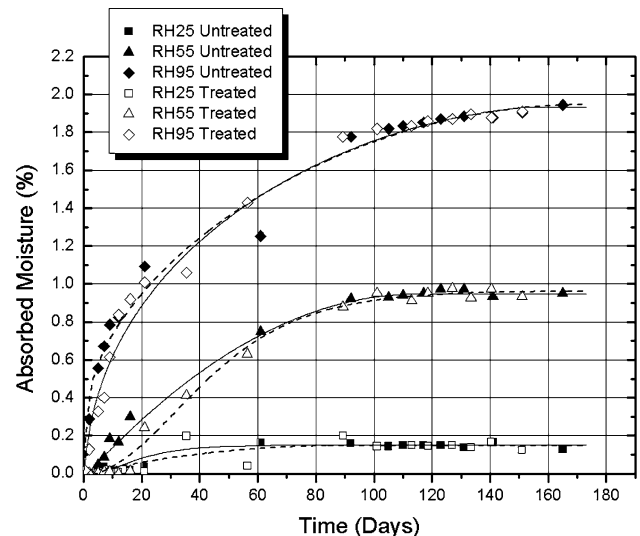

Fig. 2 Isotherms of moisture absorption for composite materials with ST carbon fiber and UT carbon fiber

reached approximately 0.15 %, an inflection point was noticed for the UT fiber specimens and then, a monotonic decrease of the tensile strength is observed. For the ST fiber, the inflection point is noticed at the same percentage of moisture absorbed. As the percentage of moisture uptake is further increased, it can be said that the tensile strength remains almost constant for the ST fibers. A similar behavior is observed in elastic modulus (see Fig. 4). A rapid decrease in elastic modulus for UT fiber is noticed at low moisture absorption content (~ 0.16 %). After that, monotonic reduction in elastic modulus is observed. For ST fiber a slow decrease is observed when the moisture absorbed reaches approximately 0.8 %. Higher content to 0.8 % the elastic modulus remains almost constant.

The effect of moisture absorption on the mechanical properties of the untreated CFRE laminates is attributed mainly to a plasticization of the epoxy matrix evidenced by a reduction of its glass-transition temperature, T_g (see Fig. 5). According to some authors [2, 24–28], the degradation of the mechanical properties of CFRE laminates due to moisture absorption is associated at the early stages, to the plasticization to the epoxy matrix and then, to a micromechanical damage induced by the absorbed moisture at the interface [29].

The micro structure of the interphase in a composite material plays a large role in the moisture diffusion process. The effects of absorbed moisture on the interfacial region could be detrimental to the interfacial strength between the fiber and the epoxy matrix and thus to the performance of the composite. Moisture-induced swelling reduces the mechanical interlocking between the fiber and the matrix that evolves during the cooling down of the sample because of the difference in thermal expansion
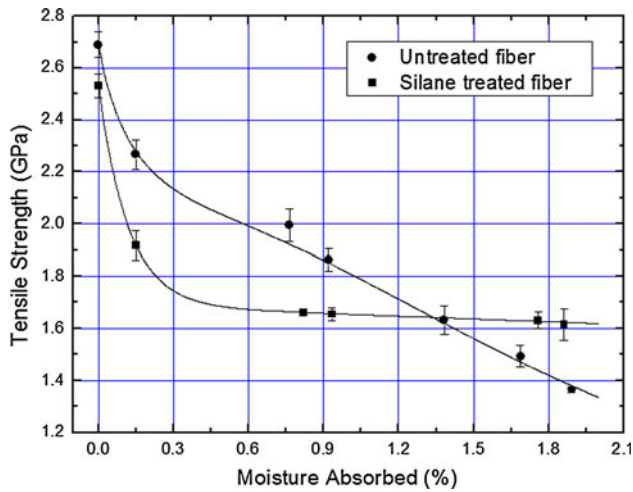
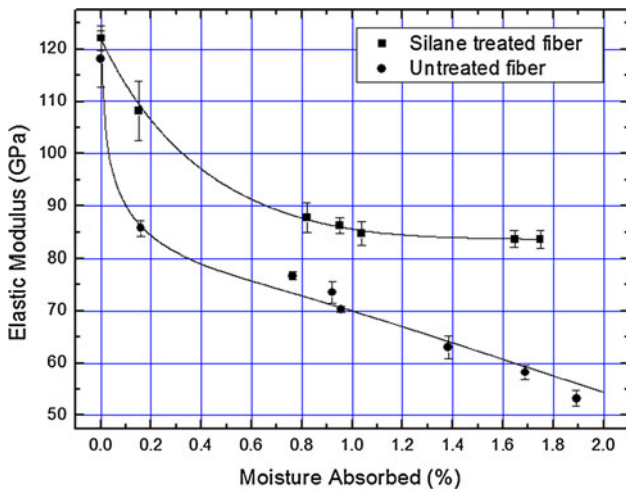**Fig. 3** Tensile strength as a function of absorbed moisture

Fig. 4 Elastic modulus as a function of absorbed moisture

Fig. 5 Graph of the T_g of the epoxy matrix as a function of absorbed moisture

strains and considers orthotropic fibers of the transversely isotropic class. The interfacial shear stress τ_{xy} is given by Eq. 2

$$\tau_{xy} = -4.75\mu A_1 \varepsilon_0 \bar{x} e^{-4.75\bar{x}}, \tag{2}$$

where A_1 is given by Eq. 3

$$A_1 = \left\{ E_{1f}\left(1 - \frac{\bar{\varepsilon}_{1f}}{\varepsilon_0}\right) + \frac{4k_f G_m v_{12f}}{(k_f + G_m)} \left[(v_{12f} - v_m) + \frac{(1 + v_m)\bar{\varepsilon}_m - \bar{\varepsilon}_{2f} - v_{12}\bar{\varepsilon}_{1f}}{\varepsilon_0} \right] \right\} \tag{3}$$

And, $\bar{x} = x/L_c$, where x is the position along the fiber-matrix interface, L_c is the fiber fragment critical length measured from the SFFT for samples subjected to each value of absorbed moisture, ε_0 is the applied far-field strain, μ and K_f given by Eqs. 4 and 5, respectively:

$$\mu = \left(\frac{G_m}{E_{1f} - 4v_{12f}G_m} \right)^{\frac{1}{2}} \tag{4}$$

and

$$K_f = \frac{E_m}{2\left(2 - \frac{E_{2f}}{2G_{2f}} - \frac{2v_{12f}^2 E_{2f}}{E_{1f}}\right)} \tag{5}$$

E_{1f} denotes the fiber axial elastic modulus, v_{12f} the longitudinal Poisson's ratio of the fiber, and G_m, denotes the matrix shear modulus. Moisture strains are indicated by overbars, E_{2f}, G_{2f}, and K_f are the radial elastic modulus, shear modulus, and the plane-strain bulk modulus of the fiber, respectively, and E_m is the elastic modulus of the matrix. The values of these parameters used in the calculation are given in Tables 1 and 2.

Figure 6 shows maximum values for the interfacial shear strength as a function of absorbed moisture calculated using Eq. 2. It is observed in Fig. 6 that, before

coefficients between two constituent materials. Thus, swelling could cause significant changes in the internal stress state in the interphase region. Reductions in T_g due to absorbed moisture could also degrade the interphase region, particularly if the wet T_g of the interphase is exceeded in service [27]. These types of deleterious effects can lead to reductions in fiber-matrix adhesion and even failure at the fiber-matrix interphase, which could then cause the formation and propagation of micro-cracks and other damage mechanisms, and therefore, lead to reduction in composite performance [4].

In order to determine the fiber-matrix interfacial shear strength (τ_{xy}) as a function of the absorbed moisture, a micromechanical model proposed by Whitney and Drzal [30] was used. The model is based on the superposition of the solutions to two axisymmetric problems, an exact far-field solution and an approximate transient solution and also includes the effects of expansional hygrothermal
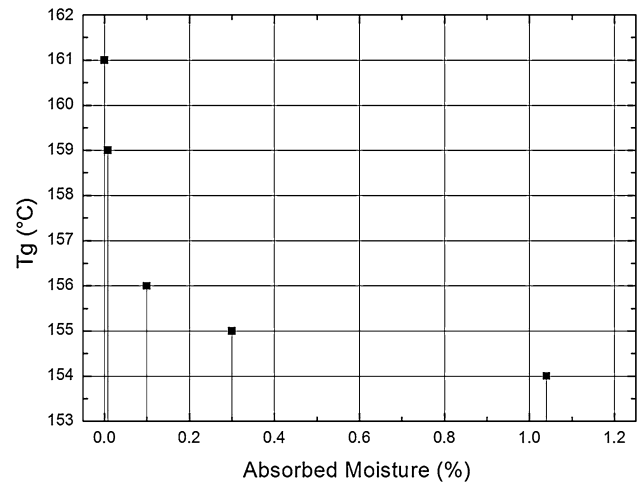
moisture conditioning, that the IFSS of the ST carbon fiber sample was approximately 1.3 times higher than that of UT carbon fiber. According to Lee and Peppas and Cauich-Cupul et al. [24, 27], the higher value of the IFSS of ST the carbon fiber sample can be explained by the surface treatment process. The fiber surface treatment effects can include removal of fiber surface defects, increase of effective surface area of the fiber, and provide strong covalent chemical bonding between the oxidized surface functional groups and epoxy resin. It is also shown in Fig. 6 that as the moisture absorption increased from 0 to 1.89 %, the IFSS decreases 35 % for UT carbon fiber and 29 % for ST carbon fiber. These results imply that the improved moisture resistance resulting from the fiber surface treatment with a coupling agent can be explained by an improvement of the fiber-matrix adhesion. It has been reported [27, 33] that the coupling agent builds chemical bonds (silanol bonds) and hydrogen bonds, which reduce the moisture-caused fiber-matrix debonding. The enhanced adhesion leads to distinctly improved mechanical properties and to a reduced dependence of the properties on humidity under tensile loading. Furthermore, in the case of the UT carbon fibers, the IFSS curve shows three distinct regions. First a sharp decrease from 0 to 0.16 % absorbed moisture, then it decreases almost linearly for absorbed moisture values of 1.37 % and then, the slope decreases again for higher moisture values. A similar behavior was observed for IFSS samples subjected to a thermal environment [26].

The water in an epoxy resin can be classified into two types of bound water according to their activation energies for desorption. Retained water molecules which are easily removed by thermal desorption at lower temperatures are consistent with a so-called Type I bound water complex and involves water molecules forming a single hydrogen bond and or dispersion bonding with the epoxy resin network. Moreover, retained water molecules which are considerably more difficult to remove by thermal desorption are referred to as a Type II bound water complex and results from water molecules forming multiple hydrogen

Table 2 Fiber and matrix material properties

Property	Epoxy resin	Carbon fiber
E_1 (MPa)	1671	241
E_2 (MPa)	1671	21
v_{12}	0.35	0.25
G_{23} (MPa)	619	8.3
$\alpha_1(10^{-6}\ °C^{-1})$	68	−11
$\beta_1(10^{-6}\ M^{-1})$	0.33	–

bonds with the resin network. Higher temperatures are required to remove Type II bound water from the epoxy resin network. The bonding complex of the multi-site/interconnected model corresponds to the Type II bound water which has higher activation energy and is harder to remove by desorption. Type I bound water diffuses into the epoxy network and breaks the initial inter-chain Van der Waals force resulting in the increase of chain segment mobility and swelling. As the amount of the Type I bound water is dominant in the water sorption process, it readily plasticizes the epoxy resins. Water molecules which form multi-site interconnected bond complexes (Type II) do not contribute significantly to plasticization of the resin [31, 32]. Moreover, these bond complexes create bridging between chain segments resulting in (pseudo crosslinking) secondary crosslinking. The formation of the Type I bonded water occurs readily in the moisture sorption process, particular at low temperature hygrothermal exposure, however, the impetus to form Type II bonding is substantially less. Longer time and higher temperatures provide the stimulus for the formation of multi-site interconnected bonding. Consequently, the amount of Type II bound water increases with exposure time and temperature [33]. By other hand, the presence of the SCA form an interpenetrating network (IPN) type of molecular architecture in the fiber-matrix interphase region. A dramatic changes to network properties as matrix resin and curing agent diffuse into and cure with the cross-linked silane to form an epoxy-silane IPN. The diffusion and reaction of the silane into the

Table 1 Matrix material properties as a function of moisture content and critical fiber fragment length for untreated (UT) and silane treated (ST)

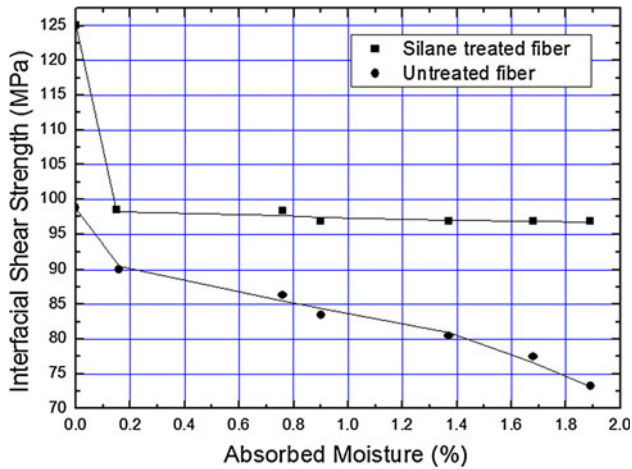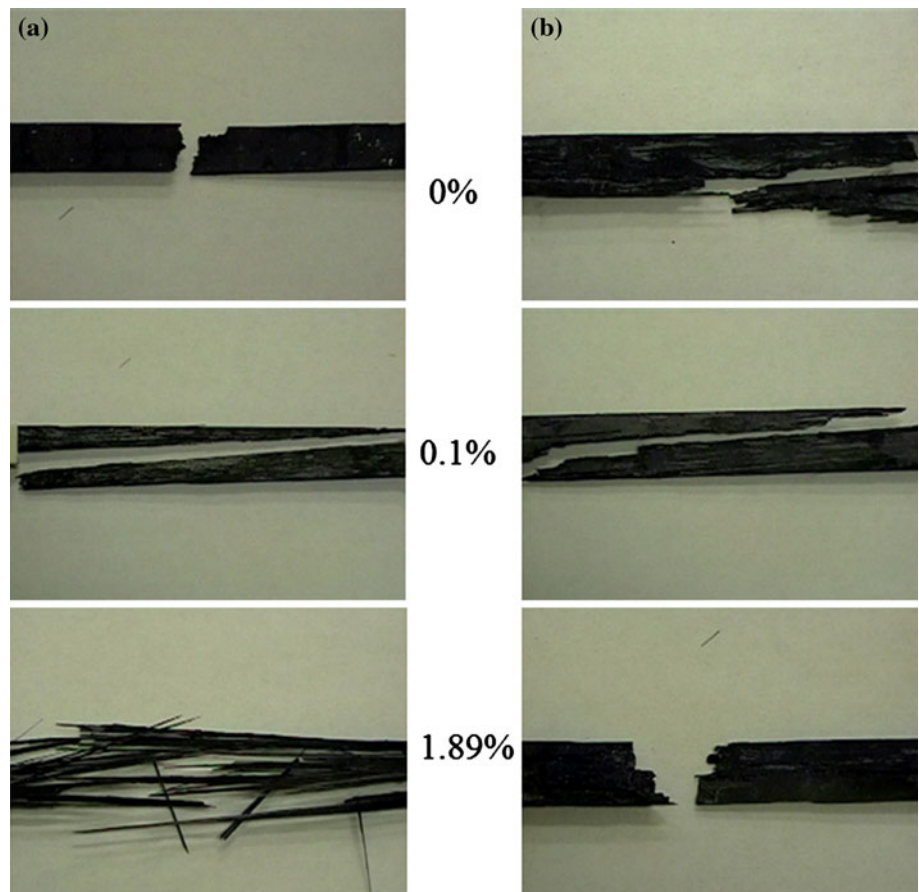| Absorbed moisture (%)	Epoxy elastic modulus (MPa)	Critical fiber fragment length (UT) (mm)	Critical fiber fragment length (ST) (mm)
0	1671	0.487	0.296
0.16	1389	0.525	0.384
0.76	1369	0.549	0.433
0.90	1369	0.587	0.473
1.37	1369	0.642	0.482
1.68	1369	0.8	0.483
1.89	1369	0.835	0.484

Fig. 6 Peak IFSS estimated using the Whitney and Drzal model for ST carbon fiber and UT carbon fiber as a function of absorbed moisture

bulk epoxy-amine matrix resin results in an interphase formation with different properties than the bulk of the matrix. Hence, the mechanical response of the interphase would be significantly different than the bulk as was expected [34].

The SCA for the surface treatment of carbon fibers has methoxy groups and a reactive rubber group. The methoxy groups of SCA molecules may form silanols during the reactions, and oxygen linkages may be formed via OH groups on the carbon fiber surfaces. Thus, improved adhesion can be accomplished by the application of this SCA onto the carbon fiber surfaces which leads to improved mechanical properties due to more efficient load transfer from the matrix to the fiber [35].

Mechanism for the observed failure behavior

The carbon fiber in CFRE laminates are impermeable to moisture, however, the epoxy matrix is very much permeable to moisture diffusion. The moisture absorption can lead to the degradation of tensile properties due to weakening of carbon fiber and epoxy matrix interface. Figure 7 shows the failure modes observed during the tensile test in carbon fiber/epoxy composites to different moisture content. As the moisture ingress to polymer composite different failure mode were observed for both UT carbon fiber and ST carbon fiber. It is important to note that when the moisture content is low (~0.1 %) no difference in failure mechanism were observed for both UT and ST carbon

Fig. 7 Failure mechanism observed in composite laminates as a function of moisture content. Row **a** UT carbon fiber and **b** ST carbon fiber

Table 3 Correlation between the physical damage and the fracture mechanism detected with AE technique

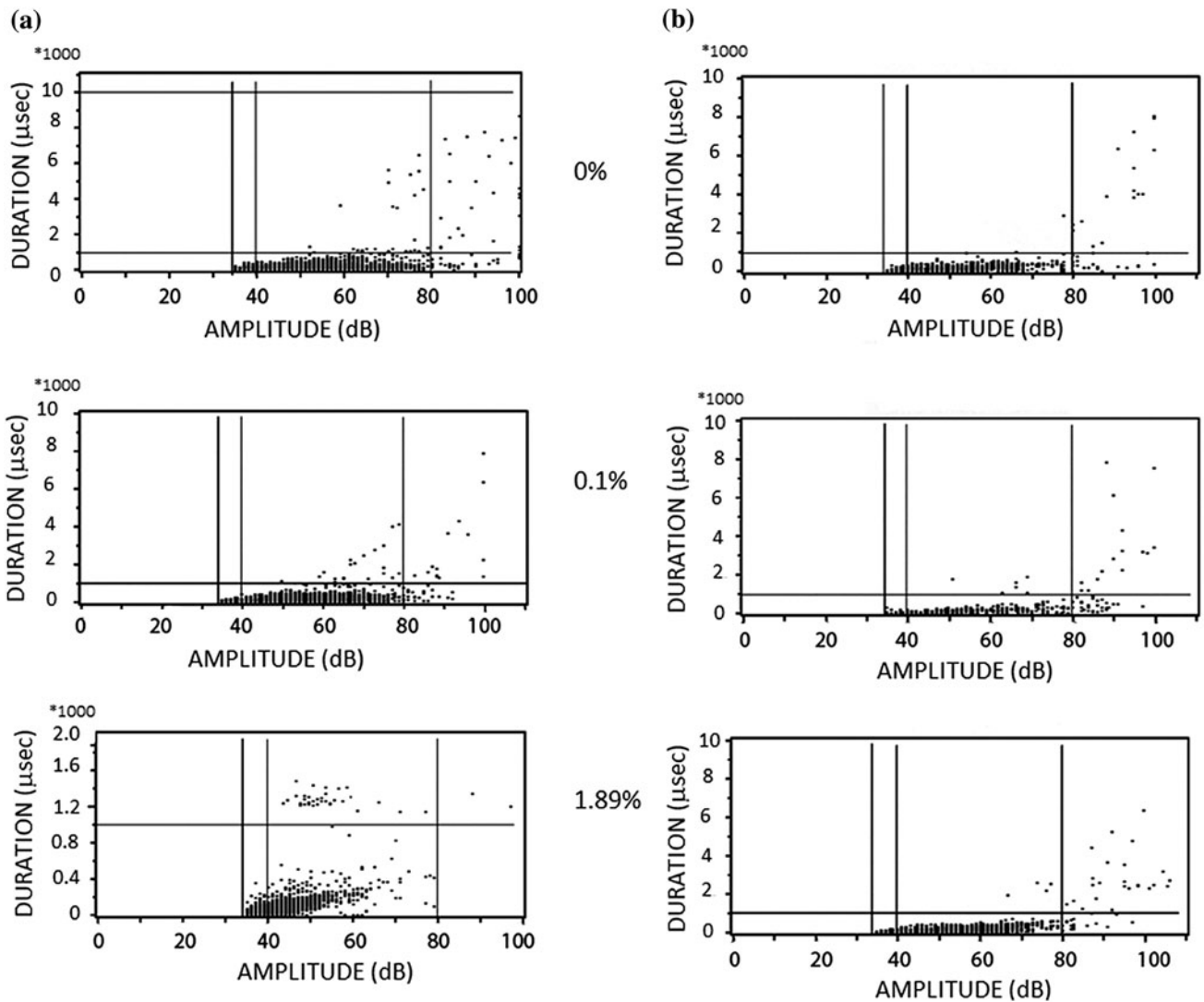| Duration	Amplitude		
	Low (35–40 dB)	Medium (40–80 dB)	High (80–100 dB)
Low (<1000 µs)	onset matrix microcrack	Propagation of matrix microcrack	–
Medium (Between 10000 µs)	–	Interfacial adhesion failure	Fiber failure
High (>10000 µs)	–	–	Propagation of macro-crack associated to delamination

Fig. 8 Acoustic emission event detected and correlated with physical damage in composite materials subjected to moisture environment. Row **a** Untreated carbon fiber and **b** Silane treated carbon fiber

fiber. The crack propagated at a 45° angle with respect to the loading axis, indicating that because of the ingress of moisture, the plasticization of the matrix led to matrix shear-yielding failure followed by fiber failure. However, for higher moisture content ($\sim$1.8 %) interfacial

debonding occurred for the untreated carbon fiber result of an "explosion" caused by a sudden release of a large amount of strain energy during the final fracture process. Meanwhile for composite materials with ST carbon fibers, the strong interface is able to sustain larger loads.

However, the decrease of the matrix yield strength is the only mechanism of crack arrest and thus, when the fibers start breaking, the strong interface at the broken ends of the fibers do not fail and a crack is initiated perpendicular to the fiber axis, resembling a "brittle" failure is observed (see Fig. 7b). The approach adopted in this study has allowed identify the damage and the failure mode during the loading of the carbon fiber reinforced polymer composite [36].

Based on the variations in amplitude and duration of the AE event, several domains were defined and correlated to the physical damage. This multi-scale approach provides evidence of a correlation between the initiation and the propagation of matrix micro-cracking and the low durations and low/medium amplitude events. The initiation and the propagation of the intra and inter-ply delamination cracks were associated to medium duration and medium/high amplitude AE events. Medium duration and highest amplitude events were assigned to fiber/bundle failure. Finally, high duration (and mainly highest amplitude) events were associated to the sudden propagation of the macro-crack including large delamination cracks [36]. A resume of several events according to its amplitude and duration are in Table 3 and the AE results are shown in Fig. 8. A failure mechanism detected in the composite material laminate with UT carbon fibers to low moisture content were an onset of micro-cracks and its propagation on the matrix and carbon fiber failure. As the humidity percentage increased in the composite, the recorded acoustic events had amplitude between 40 and 80 dB with duration between 1000 and 10000 s associated to fiber-matrix interfacial adhesion failure (see Figs. 7a, 8a with 1.89 % RH). An onset of micro-cracks and its propagation on the matrix and a carbon fiber failure were detected for ST carbon fiber. In spite of the moisture content increased to 1.89 % a very few mechanism associated with interfacial adhesion were observed, in fact the observed failure was attributed to matrix failure followed by fiber failure without any fiber-matrix debonding.

Conclusions

The effects of the moisture absorption on damage accumulation in carbon fiber–epoxy composites laminates for two different superficial carbon fiber treatment were investigated in this article. The micro structure of the interphase played a significant role in the moisture diffusion process. The effects of absorbed moisture on the interfacial region was detrimental to the interfacial strength between the fiber and the epoxy matrix and thus to the performance of the composite. The application of 3-glycidoxypropyltrimethoxysilane as coupling agent enhances the fiber-matrix adhesion because silanol bonds and hydrogen bonds are provided. The plasticization, swelling stresses and any epoxy degradation due to hydrolysis will contribute to the matrix failure mechanisms. Plasticization of epoxy matrix by moisture leads to the change in its glass-transition temperature (T_g) and affecting the mechanical response of the composite. It was observed that the tensile strength of laminates made with the SCA showed a decrease but after a moisture uptake of approximately 0.45 % remained constant. Then, the enhanced adhesion when using a SCA leads to distinctly improved mechanical properties and reduce the dependence of the properties on humidity under tensile loading.

The AE technique showed that the untreated carbon fiber failure mode was a result of fiber-matrix interfacial failure, whereas the ST CFRE laminate showed matrix and fiber and failure mode with no fiber-matrix debonding, for moisture contents up to 1.89 %.

References

1. Kyohei K, Toshimo T (1982) J Comp Mat 16:82–92
2. Gupta VB, Drzal LT (1985) J Appl Polym Sci 30:4467
3. Selzer R, Friedrich K (1997) Compos Part A-Appl S 28A:595
4. Vanlandingham MR, Eduljee RF, Gillespie JW (1999) J Appl Polym Sci 71:787
5. Nogueira P, Ramirez C, Torres A, Abad MJ, Cano J, Lopez J, Lopez-Bueno I, Barral L (2001) J Appl Polym Sci 80:71
6. Luo S, Leisen J, Wong CP (2002) J Appl Polym Sci 85:1
7. Li Y, Cordovez M, Karbhari VM (2003) Compos Part B-Eng 34:383
8. Lin YC, Chen X (2005) Chem Phys Lett 412:322
9. Fan XJ, Lee SWR, Han Q (2009) Microelectron Reliab 49:861
10. Choi HS, Ahn KJ, Nam JD, Chun HJ (2001) Compos Part A-Appl S 32:709
11. Choi HS, Ahn KJ (1995) J Korean Society Comp Mat 8:11
12. Acoustic emission testing. In: Miller RK, McIntire P, editors. Nondestructive testing handbook, vol. 5. Columbus: American Society for Nondestructive Testing, 1987
13. Netravali AN, Li ZF, Sachse WH, Wu HF (1990) In: Buckley JD (ed) Third conference on advanced engineering fibers and textile structure for composites. NASA conference publication 3082, Hampton
14. Mehan RL, Mullin JV (1971) J Comp Mat 5:266
15. DeGroot PJ, Wijnen PAM, Janssen RBF (1995) Compos Sci Technol 55:405
16. Barre S, Benzeggagh ML (1994) Compos Sci Technol 52:369
17. Kumosa M, Hull D, Price JN (1987) J Mater Sci 22:331. doi: 10.1007/BF01160589
18. Tanaka K, Minoshima K, Grela W, Komai K (2002) Compos Sci Technol 62:2169
19. Godin N, Huguet S, Gaertner R (2006) Comp Structures 72:79
20. Assarar M, Scida D, El Mahi A, Poilâne C, Ayad R (2011) Mat and Design 32:788

21. ASTM D3171: 11 Standard test methods for constituent content of composite materials, American Society for Testing Materials, Philadelphia

22. ASTM D3039/D3039M: 08 Standard test method for tensile properties of polymer matrix composite materials. American Society for Testing Materials, Philadelphia

23. ASTM E104-85 Standard, 32–34, (1985). Maintaining constant relative humidity by means of aqueous solutions. Book of ASTM Standards, Part 6. American Society for Testing Materials, Philadelphia

24. Lee MC, Peppas NA (1993) J Appl Polym Sci 47:1349

25. James AH, Sunil KK, Frank RJ (2005) Compos Sci Technol 65:1299

26. Colombini D, Martínez-Vega JJ, Merle G (2002) Polymer 43:4479

27. Cauich-Cupul JI, Pérez-Pacheco E, Valadez-González A, Herrera-Franco PJ (2011) J Mater Sci 46:6664. doi:10.1007/s10853-011-5619-0

28. Pérez-Pacheco E, Moreno-Chulim V, Valadez-González A, Rios-Soberanis CR, Herrera-Franco PJ (2011) J Mater Sci 46:4026. doi:10.1007/s10853-011-5331-0

29. Ageorges C, Friedrich K, Ye L (1999) Compos Sci Technol 59:2101

30. Whitney JM, Drzal LT (1987) In: Johnston NJ (ed) ASTM Committee D-30 on high modulus fibers and their composites, ASTM STP 937, Philadelphia

31. Zhou J, Lucas JP (1999) Polymer 40:5513

32. Tang X, Whitcomb JD, Li Y, Sue HJ (2005) Compos Sci Technol 65:817

33. Jensen RE, Palmese GR, McKnigh SH (2006) Int J Adhes Adhes 26:103

34. Iwashita N, Psomiadou E, Sawada Y (1998) Compos Part A-Appl S 29A:965

35. Siron O, Tsuda H (2000) Ann Chim Sci Mat 25:533

36. Madhukar MS, Drzal LT (1991) J Compos Mat 25:958